Functional Materials 14, No.3 (2007)

Study of nature of some defects visible in polarized light in sapphire single crystals

V.F.Tkachenko, A.Ya.Dan'ko, V.M.Puzikov, A.T.Budnikov, O.A.Lukienko, N.S.Sidelnikova, G.T.Adonkin

Institute for Single Crystals, STC "Institute for Single Crystals", National Academy of Sciences of Ukraine, 60 Lenin Ave., 61001 Kharkiv, Ukraine

Received May 29, 2007

Using the precision technique of triple-crystal X-ray diffractometry, the structure of defect parts has been studied in large-size sapphire crystals grown by the horizontal directed crystallization in reducing gas media. The optical polarization analysis has shown that the conoscopic pattern shape and color spectrum are distorted in that region and optical inhomogeneities are present as a striate structure. In the first case, the responsible defects have been established to be the small-angle dislocation twisting boundaries of the micro-blocks with disorientation angles of 0.2 to 5 angular minutes; in the second one, the macro-blocks with turning angles up to several degrees. Experimental results have been presented making it possible to establish the nature and formation kinetics of the small-angle and large-angle disorientations between the micro- and macro-blocks during the crystal growth and annealing.

Прецизионным методом трехкристальной рентгеновской дифрактометрии исследована структура дефектных частей крупногабаритных кристаллов сапфира, выращенных горизонтально направленной кристаллизацией в восстановительных газовых средах. По результатам поляризационно-оптического анализа в этих областях наблюдаются искажения формы и цветовой гаммы коноскопической картины и оптические неоднородности в виде полосчатой структуры. Установлено, что в первом случае ответственными дефектами являются малоугловые дислокационные границы кручения микроблоков с углами разориентации от 0,2 до 5 угловых минут, во втором — макроблоки с углами разворотов до нескольких градусов. Представлены экспериментальные результаты, позволяющие установить причину и изучить природу и кинетику образования малоугловых и градусных разориентаций между микро-, макроблоками в процессе роста-отжига кристалла.

To use the sapphire of (0001) basis orientation in the modern optics and optoelectronics, the material should provide a high and homogeneous structure perfection that is defined, among other factors, by the orientation, density, type and distribution character of dislocations both in the crystal volume and surface layer. Besides of the improvements in crystal growth technology, the non-destructive quality control of the blanks is to be developed. An express method for the crystal quality diagnostics is the optical polarization method making it possible to reveal the presence of macro-blocks, twins, small-angle boundaries (SABs) and even micro-stresses around the boundaries of mosaic blocks and individual dislocations [1]. When using the method, the main task is to identify reliably the defects causing the observed inhomogeneity in the polarization optical pattern. The precision triple-crystal X-ray diffractometry (TXD) [2, 3] provides substantially widened potentialities in the structure perfection studies of sapphire crystals and makes it possible to identify the structure distortion character in the crystal defect parts re-

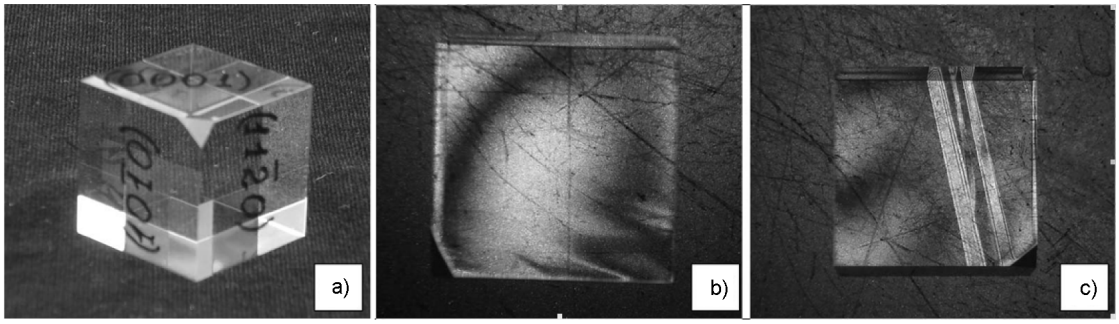

Fig. 1. Optical polarization pictures of the defect parts in {0001} oriented sapphire: general view (a), contortions (b), striate structure (c).

vealed by the preliminary qualitative optical polarization analysis.

In this work, the TXD method has been used to study the structure perfection of large-size sapphire crystals ($300\times230\times30$ mm^3 size) grown by HDC technique in reducing gas media.

An experimental crystal with the surface crystallographic orientation {0001} was grown along the $[10\bar{1}0]$ direction by the horizontal directed crystallization (HDC) technique using a standard growth unit and a high purity raw material (the characteristic impurity concentration being less than 10 ppm). Using the express optical polarization analysis, defect parts in the crystal were revealed and two cubic samples ($25\times25\times25$ mm^3) were cut out with faces oriented as {0001}, $\{10\bar{1}0\}$, and $\{11\bar{2}0\}$. Being considered in the transmitted polarized light of [0001] direction, the first sample exhibited the conoscopic pattern shape and color spectrum distortions (from here on, contortions) while the second one, optical inhomogeneities visible as a striated structure (Fig. 1b, c). The samples studied were oriented with the crystallographic planes being aligned to within $\pm0.5^\circ$ and treated (planar lapping by bound abrasive, thin lapping by boron carbide powders, mechanical and chemical polishing). The treated surface roughness R_A was about 15 Å, thus doing not influence the results of X-ray diffraction measurements carried out using an universal triple-crystal diffractometer in Cu $K\alpha_1$ radiation [2].

The structure perfection was characterized by the following parameters: the diffraction rocking curve shape (RCS), the RC angular position (Θ), the full width at half maximum (FWHM) (β), the integral reflection power (I^R). The measurements were carried out for triple planes, {0001}, $\{10\bar{1}0\}$, and $\{11\bar{2}0\}$ all the geometric surfaces of the sample being used (Fig. 1a): {0001} (the crystal head and bottom) with scanning along the $[10\bar{1}0]$ and $[11\bar{2}0]$ directions (parallel and perpendicular to the growth direction, respectively); $\{10\bar{1}0\}$, the planes perpendicular to the growth direction (nearer to and farther from the seed), with scanning along the [0001] and $[11\bar{2}0]$ directions (from the crystal surface to bottom and from the crystal center to the periphery, respectively); $\{11\bar{2}0\}$, the planes parallel to the side surface nearer to the crystal center and periphery, with scanning along the [0001] and $[1\bar{1}10]$ directions (from the crystal surface to bottom and parallel to the growth direction, respectively). The sample scanning (L-scanning) with respect to the incident monochromatic X-ray beam provided the structure perfection characteristics over the crystal cross-section with parameters $\beta(L)$, $I^R(L)$, $\Delta d/d(L)$ and evaluation of the perfection degree of the crystal volume. The $\overline{\beta}(L)$, $\overline{I^R_{\text{exp}}}(L)$ values averaged over 10 measurements are presented in Table 1. The local parts of the samples where contortions and striated structure were observed in polarized light were examined in more detail. Determined were the triple components of the turn angle, the micro (macro) block size (cross-section) as well as the structure perfection inside of the macro-blocks.

When growing the experimental crystal, the optimum spatial orientation ($\{000\bar{1}\}$ surface, $[10\bar{1}0]$ growth direction, $\{11\bar{2}0\}$ side surface), the seed shape and size and the growth conditions were selected, thus avoiding the inheritance of the seed structure defects and dislocations. The X-ray examination of such crystals have shown that the dislocations are located mainly at an angle near 90° to the growth direction and the inheritance coefficient thereof tends to zero [6].

The dislocation generation in single crystal grown from melt are due mainly to the

Table 1. Structure perfection characteristics of the sapphire sample

No.	Reflection, Θ	Sample surface	Scanning direction	Beam width at the sample, μm	$\bar{\beta}$, s	$I^R_{exp}\cdot10^5$, rad	$I^R_d\cdot10^5$, rad	$I^R_k\cdot10^5$, rad	I^R_k/I^R_d	I^R_{exp}/I^R_d	$\bar{\beta}$, s	$I^R_{exp}\cdot10^5$, rad	I^R_{exp}/I^R_d
											after annealing, taken from [5]		
1	(00012) 45°20′	Head	[10$\bar{1}$0]		12.5	1.94				3.415			
			[11$\bar{2}$0]	70	7.2	1.90				3.345			
		Bottom	[10$\bar{1}$0]		11.7	1.84	0.568	4.076	7.18	3.239	6.2	0.95	1.67
			[11$\bar{2}$0]		10.7	1.81				3.187			
2	(30$\bar{3}$0), 34.6°20′	Close to seed	[0001]		22.9	6.98	3.269						
			[11$\bar{2}$0]	89	21.5	6.85	1.90				3.345		
		Farther from seed	[0001]		25.6	6.85	2.135	33.151	15.53	3.208	12.8	3.52	1.65
			[11$\bar{2}$0]		22.0	7.06				3.307			
3	(22$\bar{4}$0) 40°21.5′	Closer to center	[0001]		10.6	1.91				3.293			
			[10$\bar{2}$0]	77	14.8	1.64				2.828	8.2	0.99	1.71
		Closer to periphery	[0001]		11.0	2.18	0.58	4.043	6.97	3.759			
			[10$\bar{1}$0]		15.2	1.94				3.345			

plastic strains resulting from the thermoelastic stresses behind the crystallization front (CF) and subsequent evolution of dislocation structures during the growth/annealing in high temperature gradients. The residual stress values and distribution depend both on the thermoelastic field character and on the plastic features of the crystal being grown. In is to note that the distribution kind and character of dislocation structures appearing at the crystal growth/annealing met the same regularities as those in the case of crystal plastic strains [7]. The X-ray examinations [6] confirm the presence of edge, screw, helicoidal dislocation structures in the HDC-grown sapphire crystals.

Consideration of RCSs for various planes in various crystallographic directions has revealed the RC blurring (Table 1) due mainly to the presence of ordered dislocation structures which may form later (under high-temperature annealing during the crystal growth) characteristic polygonal boundaries with small turn angles (1 to 5″) which give rise a splitting in RC (2 to 10 peaks) when the sample is turned near to the Bragg's reflection angle (the swinging method). Fig. 2a shows a typical RC for the {00012} reflection. The RC splitting at the half-width $\beta \sim 12''$ into 12 peaks is due mainly to the presence of polygonal boundaries with the disorientation angles $\Delta\Theta \approx 2''$. Knowing the Burgers vector value ($4.758\cdot10^{-4}$ μm), the dislocation spacing $l = b/\Delta\Theta$ can be estimated to be of about 50 μm. Knowing the beam cross-section at the sample under study and the number of the RC peaks, both the spacing of polygonal dislocation walls (about 10 μm in the samples studied) and the dislocation density ($\rho \sim 10^5$ cm^{-2}) can be estimated.

The values of the same order were obtained basing on the integral reflection coefficient I^R_{exp}. In [8], the I^R_{exp} was measured as a function of the dislocation density determined by chemical etching (the ρ error being about 15 %). The I^R_{exp} measurement at an error of about 2 % or the ρ estimation basing on the I^R_{exp}/I^R_d ratio (where I^R_d is the reflectance calculated in the dynamic approximation).

Consideration of RCS, I^R_{exp} and β provides estimation not only of ther dislocation density but also the distribution character thereof in various crystallographic planes and directions over the crystal cross-section. The strongest RC blurring is observed when the sample is scanned along [10$\bar{1}$0] directions for the {00012}, {22$\bar{4}$0} reflections and [0001] for the {30$\bar{3}$0} one (Table 1). The observed slight increase in $I^R{}_{exp}$, by about 5 % for the crystal head and by about 4 % for the bottom, indicates the same relative dislocation density both in {0001} and {10$\bar{2}$0} planes. However, it can be concluded from RCS that there is a more pronounced ordering of the polygonal dislocation boundaries in [10$\bar{1}$0] for {0001} plane along the [11$\bar{2}$0] direction and for {10$\bar{1}$0} in the [0001] one (Table 1). Thus, the RCS(L), β(L) and $I^R(L)$ values for various crystallographic planes {0001}, {10$\bar{1}$0}, and {11$\bar{2}$0} averaged over 10 measurements in

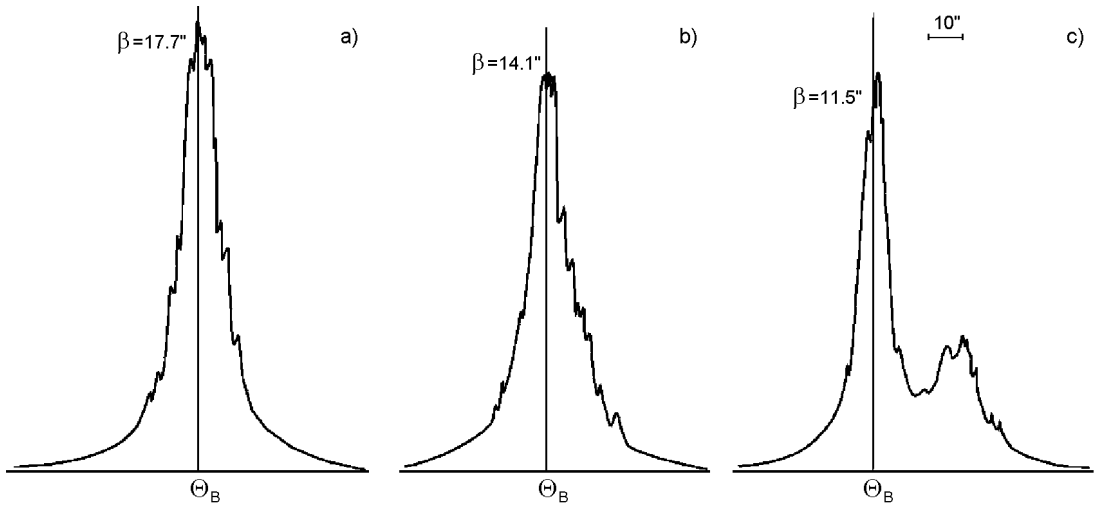

Fig. 2. Rocking curve shape, {00012} reflection, $CuK_{\alpha 1}$ radiation: near a contortion (a); beginning of contortion (b); middle of contortion (c).

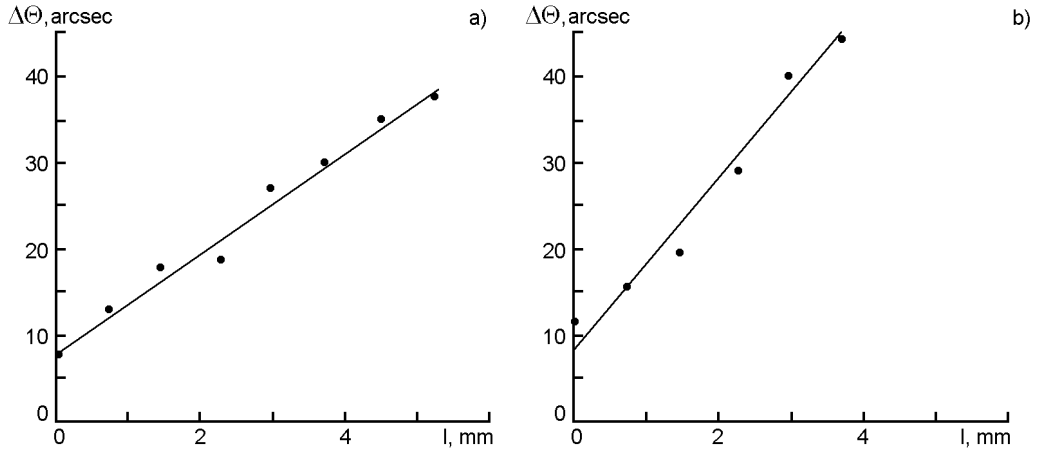

Fig. 3. Variation character of the disorientation angle ΔΘ between micro-blocks in the sample scanned along [10$\bar{1}$0] direction within the contortion region: the crystal head (a) and bottom (b).

various directions [10$\bar{1}$0] and [11$\bar{2}$0] and [0001] characterize clearly the crystal structure perfection without destroying.

When studying the crystal local regions where contortions were observed in polarized light, the defect sample part was scanned with respect to the incident X-ray beam of 8×0.05 mm^2 cross-section at 0.75 mm steps. A point near the observed optical homogeneity was selected as the starting one. In Fig. 2, presented are RCS from the {00012} reflection for scanning along the [10$\bar{1}$0] direction across the contorted region. As is seen in Fig. 2a, near the contortion the RC of about 18" half-width (β) is split into 12 peaks, that indicates the presence of polygonal boundaries with about 2″ disorientation angles and about 6 μm wall spacing. When the X-ray beam hits partially the contorted region, a RC asymmetry is observed (Fig. 2b), the β diminution down to about 14″ and the split number becomes smaller. At the further displacement, a small-angle micro-block boundary is observed with the turn angle ΔΘ≈30″ at a distance of 3.75 mm from the scan start (Fig. 2c), the ΔΘ increasing up to 40″ at the further displacement (Fig. 3). The second component of the inter-micro-block turn attains the same value as the sample is turned at 90° in its plane. There is also the third turn component when th RC is written for the {1010} plane making 90° angle with the {0001} one. Thus, the contortion observed in polarized light is

Table 2. Block structure characteristics of the sapphire sample (Fig. 1c)

No.	Crystal head				Crystal bottom		
	Θ	$\lvert\Delta\Theta_t\rvert$	Between the bloks	l, mm	$\lvert\Delta\Theta_b\rvert$	Between the bloks	l, mm,
1c	44°56′36″						
2	48°35′42″	3°39′6″	1c — 2	1.0	3°37′55″	1c — 2	1.0
3	44°33′36″	4°2′6″	2 — 3	1.5	4°14′38″	2 — 3	1.5
4	43°12′18″	1°21′19″	3 — 4	0.5	1°24′22″	3 — 4	0.5
5	44°31′30″	1°19′12″	4 — 5	2.0	1°22′37″	4 — 5	2.0
6	40°32′42″	3°58′48″	5 — 6	1.0	3°53′10″	5 — 6	1.0
7c	44°44′31″	4°11′49″	6 — 7c		3°44′24″	6 — 7c	

caused by the small-angle twisting dislocation boundary between the micro-blocks with disorientation angles of 10″ to several tens of angular seconds. The small-angle twisting boundaries are observed as a rule within the whole crystal volume where the dislocation density $\rho \geq 10^5$ cm^{-2}.

The twisting boundary is formed mainly due to the plastic straining processes resulting from relaxation of thermoelastic stresses at the CF and subsequent evolution of partially ordered dislocation walls of polygonal type during the crystal growth/annealing process. It is to note that as a crystal is grown by the HDC technique at the pulling speed up to 8 mm/h, the grown crystal is hold for about 10 h within the high-temperature zone (>1800°C) and then for more than 60 h under high temperature gradients. In those conditions, the evolution of dislocation accumulations proceeds intensely and results at end in formation of a small-angle twisting boundary of several millimeters length. Along with the contortion patterns (Fig. 1b), striation is observed in some crystals under polarized light (Fig. 1c) that points to the macro-block formation. The sample scanning with respect to the incident monochromatic beam makes it possible to determine the Bragg's reflection angle, the angular deflection and the macro-block cross-section. The measurements were done using the {00012} reflection when scanning the upper and lower crystal surfaces along the [11$\bar{2}$0] and [10$\bar{1}$0] directions and the {30$\bar{3}$0} reflection when scanning the sample surfaces perpendicular to the growth direction along the [0001] and [11$\bar{2}$0] directions.

The measured angles (Θ) and disorientation angles ($\Delta\Theta_i$) between the crystal surface and the 1st, 2nd, etc. boundaries when scanning the upper and lower crystal surfaces along the [11$\bar{2}$0] direction are presented in Table 2. The turn angles between the macro-blocks of about 1 mm^2 cross-section and several cm length are seen to amount 1 to 4°. The variation character of disorientation angle between the macro-blocks in the crystal section at $L \approx 8$ mm is shown in Fig. 4. No substantial distinctions have been revealed in the dimensions (cross-sections) and the turn angles in the upper and lower crystal parts along the [11$\bar{2}$0] direction. The measurements of the second turn components for the sample turned by 90° along the [10$\bar{1}$0] show much smaller disorientation angles between the macro-blocks (up to 5′) while the third turn component between the mosaic blocks was measured to be about $\Delta\Theta_{max} \approx 18'$. Thus, the maximum turn between the macro-blocks is observed along [11$\bar{2}$0] and is well seen in polarized light (Fig. 1c). At the same time, the main crystal part to left and to right of the macro-block region shows an insignificant distinction ($\Delta\Theta \approx 12'$).

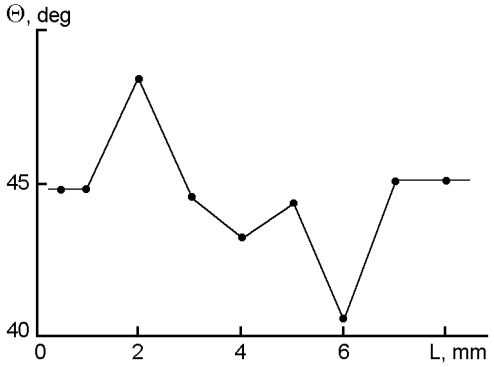

Fig. 4. Variation character of the disorientation angles between macro-blocks in the sample scanned along [11$\bar{2}$0] direction.

The about 6 mm wide region containing macro-blocks with large turn angles is formed for quite other reasons than the small-angle twisting boundaries. Perhaps the main formation cause of such macro-blocks consists in local distortions of temperature field at the CF that may result in formation of triple-dimensional nuclei (dendrites) in the melt in front of CF and the subsequent growth thereof together with the main crystal bulk. Such local CF distortions result in that a packet of macro-blocks may be formed within the grown crystal bulk; that packet has a certain width, includes a certain number of blocks and is extended as a rule over the whole crystal length. The structure perfection within such macro-blocks is characterized by the presence of small-angle twisting boundaries between micro-blocks and an increased dislocation density.

To prepare substrates satisfying the performance requirements in optoelectronics and microelectronics, sapphire should have the dislocation density $\leq 10^4$ cm^{-2}, contain neither small-angle twisting boundaries between blocks nor block structure. The current technology yields such material in amounts of 60 to 70 % of the whole crystal mass. The improvement of the defect-free material yield seems to require a modernization of the growth unit heat assemblies and transition to more "soft" crystal annealing conditions during its growing.

References

1. Ruby and Sapphire, Nauka, Moscow (1974) [in Russian].
2. V.F.Tkachenko, M.A.Rom, A.A.Babichenko, V.I.Kuznetsov, *Pribory Tekhn.Eksper.*, **2**, 277 (1992).
3. USSR Author's Cert. 1072265 (1991).
4. A.Ya.Dan'ko, V.F.Tkachenko, G.T.Adonkin et al., *Poverkhnost'*, **5**, 75 (2002).
5. A.Ya.Dan'ko, V.F.Tkachenko, N.S.Sidelnikova et al., *Functional Materials*, **7**, 251 (2004).
6. E.R.Dobrovinskaya, V.V.Kukol, V.V.Pishchik, G.M.Tsigelnitsky, *Kristallografia*, **20**, 399 (1975).
7. V.L.Indenbom, *Izv.AN SSSR, Ser.Fiz.*, **37**, 2258 (1973).
8. A.N.Belaya, E.R.Dobrovinskaya, V.V.Kukol et al., in: Single Crystals and Engineering, VNII Monokristallov Publ., 14th Issue (1976), p.49 [in Russian].

Дослідження природи деяких дефектів монокристалів сапфіру, що є видимими у поляризованому світлі

В.Ф.Ткаченко, О.Я.Данько, В.М.Пузіков, О.Т.Будніков, О.О.Лукієнко, Н.С.Сідельнікова, Г.Т.Адонкін

Прецизійним методом трьохкристальної рентгенівської дифрактометрії досліджено структуру дефектних частин великогабаритних кристалів сапфіра, вирощених горизонтально спрямованою кристалізацією у відновних газових середовищах. За результатами поляризаційно-оптичного аналізу у цих областях спостерігаються перекручування форми й колірної гами коноскопічної картини й оптичні неоднорідності у вигляді смугастої структури. Установлено, що у першому випадку відповідальними дефектами є малокутові дислокаційні границі крутіння мікроблоків з кутами розорієнтації від 0,2 до 5 кутових хвилин, у другому — макроблоки з кутами розворотів до декількох градусів. Представлено експериментальні результати, що дозволяють установити причину й вивчити природу й кінетику утворення малокутових і градусних розорієнтацій між мікро-, макроблоками у процесі росту-відпалу кристала.